Vehicular Communications 3 (2016) 12–20

Contents lists available at ScienceDirect

Vehicular Communications

www.elsevier.com/locate/vehcom

Decode-and-Forward cooperative vehicular relaying for LTE-A MIMO-downlink

Mohamed Feteiha [a,b,*], Hossam S. Hassanein [a]

[a] Telecommunications Research Lab, School of Computing, Queen's University, Kingston, ON, K7L 2N8 Canada
[b] Networks and Distributed Systems Department, Informatics Research Institute, City of Scientific Research and Technological Applications, Alexandria 21934, Egypt

ARTICLE INFO

Article history:
Received 1 December 2014
Received in revised form 15 May 2015
Accepted 26 November 2015
Available online 15 December 2015

Keywords:
Cooperative communications
MIMO
Performance analysis
Vehicular relaying
Mathematical modelling
Channel diversity

ABSTRACT

Cooperative multiple-input multiple-output technology allows a wireless network to coordinate among distributed single or multiple antenna deployments and achieves considerable performance gains compared to those provided by conventional transmission techniques. It promises significant improvements in spectral efficiency and network coverage and is a major candidate technology in various standard proposals for the fourth-generation wireless communication systems. We propose to use cooperative multiple antenna deployment links in Long Term Evolution-Advanced networks where vehicles act as relaying terminals using Decode-and-Forward relaying. To maintain orthogonality of signals, we deploy a modified Alamouti-based Space–Time Block Coding technique. Our approach allows exploitation of the multiplexing capability and spatial diversity of typical multiple antenna schemes in distributed way. We further contribute by deriving error rate, diversity gain and outage probability closed form expressions as a benchmark to assess our analysis and future research studies. Our findings indicate that significant diversity gains and reduced error rates are achievable. As well, a noticeable reduction in the required transmitting power, and an increase in coverage distance are observed compared to traditional single antenna deployments.

1. Introduction

The evolution of fourth generation (4G) mobile communication has enabled new services and usage models with higher efficiency networks. 4G systems support a wide range of applications that require high data rates and reliable transmission. To meet this demand, wireless communication system designers need to advance and optimize network performance in terms of better link reliability, fewer dropped connections and longer battery life. Long Term Evolution-Advanced (LTE-A), which was ratified by the International Telecommunication Union (ITU) as an IMT-Advanced 4G technology in November 2010, has adopted relaying for cost-effective throughput enhancement and coverage extension. The utilization of multi-hop relaying techniques aims at increasing network performance without the need to undergo costly network infrastructure expansion [1,2].

Concurrently, the continuous increase of mobile data traffic has created a substantial demand for high data rate transmission over 4G mobile networks. The uplink power and efficiency constrains are studied in [3,4]. In [3], two power-efficient schedulers for mixed streaming services are presented to minimize transmission power for all users in LTE uplink systems. Simulation results show that the proposed schedulers offer a significant transmission power reduction for the LTE link. In [4], a framework for energy efficient resource allocation in multiuser synchronous constraints is presented. Using this framework, the authors formulate the optimal margin adaptive allocation problem, and proposed two suboptimal approaches to minimize average power allocation required for resource allocation for LTE links while attempting to reduce complexity. For the multiple-input multiple-output (MIMO) downlinks, the authors in [5] focus on minimizing the long-term average power consumption of a transmitter providing Quality of Service (QoS) enabled traffic to a receiver. While both the transmitting and receiving stations are equipped with multiple antennas. The designed policy exploits queue state information to schedule traffic while meeting throughput and loss constraints.

Recently, vehicular networks cooperative relaying has been proposed to extend coverage, enable ad-hoc connectivity and enhance link reliability. Cooperative communication has been proposed for vehicular networks through distributed spatial diversity by making use of vehicles equipped with low elevation antennas, and short and medium range wireless communication technologies. The ad-

* Corresponding author.
E-mail addresses: feteiha@cs.queensu.ca (M. Feteiha), hossam@cs.queensu.ca (H.S. Hassanein).

http://dx.doi.org/10.1016/j.vehcom.2015.11.002
2214-2096/

vantages of vehicular relaying networks include the abundant energy and computing power, the predictable movement that is in the most common cases limited to roadways, the availability of positioning systems and map-based technologies, and the frequent availability of travelling vehicles. Hence, vehicular relaying is envisaged to be a key technology enabling significant network growth in the coming years. Most vehicular wireless communication measurement campaigns have focused on single-antenna applications, leading to the development of single-input single-output (SISO) systems, e.g., [6–9] and the references within. However, only a few measurement campaigns [10–12] have so far been conducted for MIMO Vehicular channels. For simplicity assumptions, multiple uncorrelated Rayleigh fading processes often implemented MIMO channel models.

It is well recognized that MIMO wireless systems can improve link performance and spectral efficiency by utilizing diversity and multiplexing gains [10,13]. For MIMO channels it is very likely that correlated channel fading coefficients appear if the transmit antennas of the same transmitter/receiver are within a range of a few wavelengths. This leads to a degradation of the error rate performance as diversity is lost. To overcome this phenomenon, Space–Time Block Coding (STBC) [14] is used to enforce orthogonality of the transmitted signals. This in turn provides the ability to extract full signal diversity. STBC can achieve an optimal tradeoff between multiplexing gain and diversity gain, which means such codes can achieve the optimal diversity gain [15]. Provisioning practical STBC for cooperative relay channels is fundamentally different from STBC for MIMO link channels and is still an open and challenging area of research. Apart from practical STBC for the cooperative relay channel, the formation of virtual antenna arrays using individual terminals distributed in space requires a significant amount of coordination. Specifically, involves distributed transmissions while synchronizing at the packet level amongst the different communicating nodes. In this paper, we make use of a modified STBC-MIMO deployment for dual-hop cooperative systems.

Although the expectations for this emerging technology are set very high, many practical challenges still remain unsolved. In most practical scenarios in such high mobility communication, inter-symbol interference (ISI) due to the broadband nature of the system introduces frequency-selectivity, and Doppler spreads resulting in time-selectivity. Within the research of cooperative diversity, one commonly used technique for the transmission between a source and a destination through relays is Decode-and-Forward (DF). In DF, relays first decode the received signal, re-encode it, and then transmit the re-encoded signal to the destination. Beside DF, the most common relaying strategy is amplify-and-forward (AF). AF simply amplifies and retransmits the signal without decoding. It was shown in [16] that the DF protocol achieve higher ergodic (mean) capacity than the AF. A similar conclusion was found in [17] for the ergodic capacity of MIMO multi-hop relay systems. From [16] and [17] we conclude that while the AF protocol is better for uncoded systems (where the error propagation effect outweighs the noise amplification), the opposite is true for systems using powerful capacity-approaching codes, where DF outperforms AF. DF also avoids error propagation in practice, where a relay node can decide that an incorrect decision has been made through cyclic redundancy check (CRC) deployment.

In this paper, we study cooperative vehicular relaying for a downlink LTE-A communication session, using a multiple antenna deployment installed at a transmitting cellular base-station (eNodeB/BS) and a designated receiving end vehicle through a highway traffic. The source and destination nodes are equipped each with two antennas while the relay node has a single transmit/receive antenna. Note that a single antenna at the relaying vehicle allows maintaining the basic minimum required power and processing capabilities without the need for extra hardware deployment. As mentioned above, Alamouti-type STBC [14] is modified and used across the two transmit antennas of the source node and the two receive antennas at the designated vehicle.[1] Since time-selectivity destroys the orthogonality of STBC, we employ digital phase sweeping (DPS) to overcome the degrading effects of time-selectivity. DPS converts space–time time-selective channels into a single faster time-selective channel [18]. We further contribute by

1) deploying an effective pre-coding transmission scheme and a MIMO encoding technique for the model under consideration (illustrated in Table 1) that significantly increase diversity gains and reduce error rates;

2) the derivation of closed-form formulae for the error performance rate, diversity gains and outage probability as a benchmark to assess our analysis and future research studies of such an approach; and

3) demonstrating the performance gains of the proposed approach, analytically and through simulation, compared to the traditional approaches.

In addition to higher diversity and improved levels of error rates, our transmission scheme shows tight performance compliance to similar ideal stationary flat-fading scenarios even under high mobility and selective fading.

The paper is organized as follows: In Section 2, we present the pre-coded cooperative system model along with the vehicular fading channel. In Section 3, we provide diversity gain analysis through derivation of the Pairwise Error Probability (PEP); further we derive the outage probability. In Section 4, we present numerical and simulation results for the error rate performance, the diversity gains and the coverage distance advantages of our proposed scheme. We conclude our findings in Section 5.

Notations. $(.)^{\mathrm{T}}$, $(.)^*$ and $(.)^{\mathrm{H}}$ denote transpose, conjugate and Hermitian operations, respectively. $\mathbb{E}[.]$, $|.|$ and $\otimes$ denote expectation, absolute value and Kronecker product, respectively. $[\mathbf{H}]_{k,m}$ represents the (k,m)-th entry of $\mathbf{H}$. $\mathbf{I}_N$ indicates an $N \times N$-size identity matrix. $\mathbf{0}$ represents all-zeros matrix with proper dimensions. $\lceil . \rceil$ and $\lfloor . \rfloor$ denotes integer ceil and integer floor operations, respectively. $*$ is the convolution operator. x, i, j, k are dummy variables. $F(.)$ and $f(.)$ are the cumulative distribution function (CDF) and probability density function (pdf) for a given random variable, respectively. **Bold** letters/symbols denote matrices and vectors.

2. System model

As illustrated in Fig. 1, we consider a highway traffic scenario, where the relay and destination vehicles are assumed to be travelling in the same direction with similar speeds and communicating with a fixed BS through an LTE-A downlink session.[2] In this scenario, source-to-destination and source-to-relay links are modelled by a doubly-selective channel due to the relative velocity between the communicating nodes. On the other hand, since the relative Doppler frequency of the relaying and destination vehicles travelling in the same direction with similar speeds becomes nearly zero, the relay-to-destination link can be modelled by a time- and frequency-flat channel. In this section, we first describe the vehicular channel model and then present the pre-coded cooperative MIMO scheme under consideration. There are mainly two approaches to handle cooperative communications. The first approach involves adaptive transmission in which one or more transmission parameters (coding, modulation, power, etc.) are varied

[1] Extension to more than two antennas is straightforward with a more cumbersome notation.

[2] A scheme similar to the one in [19] can be used to ensure such relay selection.

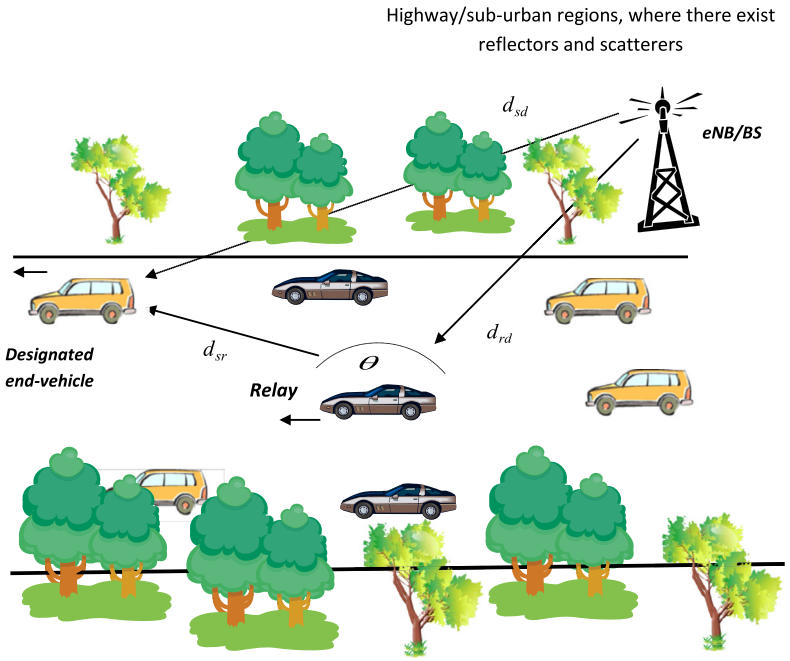

Fig. 1. Cooperative best-relay selection model in a highway/suburban area with 2×2 MIMO deployment.

according to the channel conditions. This builds on a closed-loop implementation in which feedback from the receiver to the transmitter is required. The second approach is the use of either outer coding or pre-coding. These are open-loop implementations which do not require feedback. Such techniques are particularly useful over time-varying channels where reliable feedback is difficult to obtain. In our paper, considering the time-selective nature of the vehicular system under consideration, we used the linear constellation pre-coding (LCP) approach. Taking this into consideration, we will build our communication scheme over orthogonal transmission protocol, cooperative relaying, as well as outer and linear signal pre-coding.

2.1. Channel model

To reflect the relay geometry, we consider an aggregate channel model which takes into account both path-loss and small-scale fading. The path loss is proportional to d^{α} where d is the propagation distance and α is the path loss coefficient. Let d_{sd}, d_{sr} and d_{rd} denote the distances of source-to-destination (S $\rightarrow$ D), source-to-relay (S $\rightarrow$ R), and relay-to-destination (R $\rightarrow$ D) links, respectively, and θ be the angle between lines S $\rightarrow$ R and R $\rightarrow$ D. Normalizing the path loss in S $\rightarrow$ D to be unity, the relative geometrical gains are defined respectively as $G_{sr} = (d_{sd}/d_{sr})^{\alpha}$ and $G_{rd} = (d_{sd}/d_{rd})^{\alpha}$. The ratio G_{sr}/G_{rd} reflects the effect of relay location. A more negative ratio translates into closer proximity of the relay to the destination terminal.

The Jakes model [20] assumes an isotropic rich scattering around the mobile receiver antenna and builds upon a *single-ring model*. In this model, the angles of arrival of the waves arriving at the receiving antenna are uniformly distributed. This single ring model is generally used for cellular systems that typically involve a stationary base station antenna above roof-top level unobstructed by the local scatterers. When the transmitter vehicle and/or the receiver vehicle are in motion, the Doppler phase shift, i.e. the amount of change in the frequency due to the vehicles' relative mobility, must be taken into account. In highly scattered areas, there are a large number of paths along with the absence of a dominating line-of-sight (LOS) path. Central Limit Theorem suggests that the complex fading coefficient can be modelled as zero-mean complex Gaussian. Therefore, the envelope of the channel follows a Rayleigh distribution while the phase is uniformly distributed [21]. In vehicular communication, the antenna is close to the ground level (1.5–2.5 m), and is dynamic with higher speed and variation; which requires considering the local scattering around the vehicular antenna. In [22], Akki and Haber consider a scattering model surrounding the mobile terminals with omni-directional antennas; assuming two communicating terminals moving with velocities v_1 and v_2. For this mobility scenario, each path will be subject to separate Doppler shifts. For the short-term fading model, we adopt the double-ring channel model of [22] which assumes that scatterers lay uniformly over two rings around the two vehicles. The envelope of this channel follows a Rayleigh distribution, however its second order statistics differ from Jakes' model (traditionally used in cellular communications). The corresponding autocorrelation function in the double-ring channel model is given by

$$C(\tau) = \sigma^2 J_0\left(\frac{2\pi}{\lambda} v_1 \tau\right) J_0\left(\frac{2\pi}{\lambda} v_2 \tau\right) \tag{1}$$

The maximum Doppler shift due to the relative motion of the two vehicles is given by $f_{D_m} = [v_1 \cos(\vartheta_1) + v_2 \cos(\vartheta_2)]/\lambda$, where λ is the wavelength of the carrier frequency with ϑ_1 and ϑ_2 representing the angle of incidence of the signal on the first and second vehicles, respectively. Note that in a vehicular channel there are several instantaneous velocities due to acceleration/decelerations. Maximum Doppler shift f_{D_m} is calculated based on the maximum velocities experienced. We can further define the Doppler spread given by $f_d = 1/T_d$, where T_d is the coherence time of the channel. In addition to time-selectivity, the channel is subject to frequency-selectivity quantified through delay spread τ_d.

2.2. Transmission model

We adopt the orthogonal cooperation protocol and DF relaying [23]. In the broadcasting phase, the BS sends its signal to the relay and the destination vehicles. In the relaying phase, the relay vehicle properly decodes its received signal and forwards the resulting signal (only if correct) to the destination. The destination makes its decision based on the maximum likelihood (ML) detection of

Table 1
Encoding for STBC cooperative transmission.

	(Phase 1) broadcast-1	(Phase 2) broadcast-2	(Phase 3) relaying-1	(Phase 4) relaying-2
Tx antenna-1	transmit $\mathbf{s}(n-1)$	transmit $-\mathbf{s}^*(n)$	*idle*	*idle*
Tx antenna-2	transmit $\mathbf{s}(n)$	transmit $\mathbf{s}^*(n-1)$	*idle*	*idle*
Relay antenna	receive $\mathbf{y}_{sr}(n-1)$	receive $\mathbf{y}_{sr}(n)$	transmit $\tilde{\mathbf{y}}_{sr}(n-1)$	transmit $\tilde{\mathbf{y}}_{sr}(n)$
Rx antenna-1	receive $\mathbf{y}_{sd,1}(n-1)$	receive $\mathbf{y}_{sd,1}(n)$	receive $\mathbf{y}_{rd,1}(n-1)$	receive $\mathbf{y}_{rd,1}(n)$
Rx antenna-2	receive $\mathbf{y}_{sd,2}(n-1)$	receive $\mathbf{y}_{sd,2}(n)$	receive $\mathbf{y}_{rd,2}(n-1)$	receive $\mathbf{y}_{rd,2}(n)$

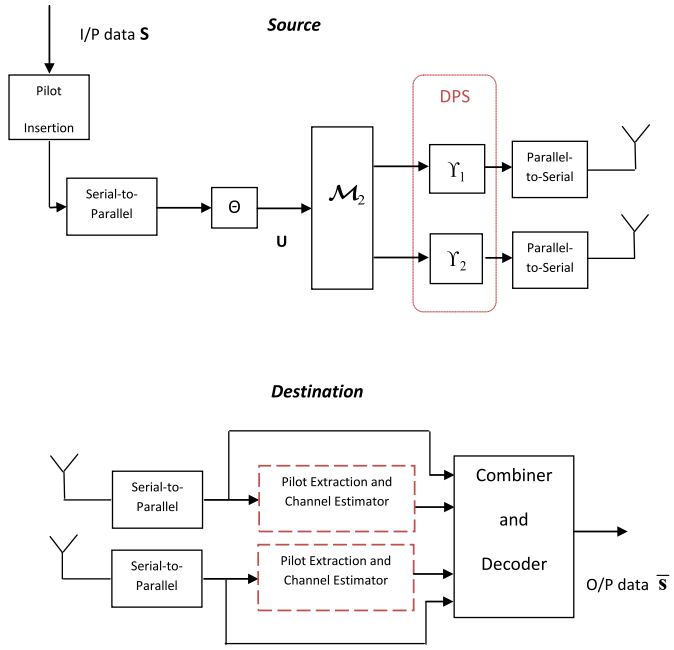

Fig. 2. Alamouti-code based MIMO cooperative transmission scheme.

the two received signals. Fig. 2 shows a block diagram for the source and the destination with $\mathcal{M}_2$ denoting the STBC matrix. As summarized in Table 1, we use four transmission phases. For ease of presentation, we first provide the received signals for the single antenna-to-antenna links. We consider a pre-coded cooperative scheme as shown in Fig. 2, the input data blocks (generated from an M-QAM constellation) of length N_t are divided into shorter sub-blocks of length N_s ($N_s \leq N_t$). Let $\mathbf{s}(n)$ denote sub-block (n) which will be the input to the linear pre-coder $\boldsymbol{\Theta}$ of size $N_s \times N_t$. We use the pre-coder proposed in [24], which ensures maximum diversity over doubly-selective channels and eliminates the inter-block interference (IBI) term. The pre-coder is given by $\boldsymbol{\Theta} = \mathbf{F}_{P+Q}^{\mathrm{H}}\,\mathbf{T_1} \otimes \mathbf{T_2}$ where $\mathbf{F}_{P+Q}^{\mathrm{H}}$ is a $(P+Q)$-point IFFT matrix, $\mathbf{T}_1 := [\mathbf{I}_P,\ \mathbf{0}_{P\times Q}]^{\mathrm{T}}$ and $\mathbf{T}_2 := [\mathbf{I}_Z,\ \mathbf{0}_{Z\times L}]^{\mathrm{T}}$. Here, $P \geq 1$ and $Z \geq 1$ are the pre-coder design parameters such that $N_s = PZ$, $N_t = (P+Q)(Z+L)$. The number of resolvable multipath components is given by $L = \lceil \tau_d / T_s \rceil$ and the number of Doppler shifts experienced over the data block is given by $Q = \lceil N_t T_s f_{D_m} \rceil$.

Based on the Basis Expansion Model (BEM), a discrete-time baseband equivalent channel for the doubly-selective channel under consideration is given by a time-sampled OFDM signal converted into frequency domain by implementing a discrete Fourier transform (DFT). The DFT renders a discrete finite sequence of complex coefficients, which are given by

$$s(\ell) = \frac{1}{\sqrt{N}} \sum_{k=0}^{(N-1)} x(k)\, e^{-jw_k} \tag{2}$$

where $w_k = 2\pi \ell k / N$, while $x(k)$ is the modulated symbol, and $n = 0, \ldots, N-1$. The BEM can be used to represent a discrete-time baseband equivalent channel for the doubly-selective channel associated with this type of mobility, and given by

$$h_B(\ell; l) = \sum_{q=0}^{Q} h_q(n; l)\, e^{jw_q},\ l \in [0, L] \tag{3}$$

where $w_q = 2\pi\,\ell\,(q - Q/2)/N_s$ are the finite Fourier bases that capture the time variation, $h_q(n; l)$ is zero-mean complex Gaussian. Here, ℓ denotes the serial index for the input data symbols. The block index is given by $n = \lfloor \ell / N_t \rfloor$. Define $\mathbf{H}_{sd,q}^{(0)}$, $\mathbf{H}_{sr,q}^{(0)}$ and $\mathbf{H}_{rd,q}^{(0)}$ as the lower triangular Toeplitz channel matrices with entries given by (3). Let L_{sd}, L_{sr} and L_{rd} denote the channel multipath orders for the S $\rightarrow$ D, S $\rightarrow$ R, and R $\rightarrow$ D links, respectively. Further, let Q_{sd}, Q_{sr} and Q_{rd} denote the number of resolvable Doppler components and define $\mathrm{Q} = \max(Q_{sd}, Q_{sr}, Q_{rd})$. In the broadcasting phase, the received signals at the relay can be expressed in matrix form as

$$\begin{aligned}\mathbf{y}_{sr}(n) &= \sqrt{G_{sr}E_s} \sum_{q=0}^{\mathrm{Q}} \mathbf{D}\left(w_q\right)\mathbf{H}_{sr,q}^{(0)}(n)\,\mathbf{u}(n) + \mathbf{n}_{sr}(n) \\ &= \sqrt{G_{sr}E_s}\,\boldsymbol{\Phi}(n)\,\mathbf{h}_{sr}(n) + \mathbf{n}_{sr}(n)\end{aligned} \tag{4}$$

where $\mathbf{u}(n) = \boldsymbol{\Theta}\mathbf{s}(n)$ is the transmitted data block, E_s is the modulation symbol energy, $\mathbf{D}\left(w_q\right) := \mathrm{diag}\left[\,1,\ \ldots\ \exp\left(jw_q\,(N_t-1)\right)\right]$ and $\mathbf{n}_{sr}(n)$ is the additive white Gaussian noise (AWGN) vector with entries of zero mean and $N_0/2$ variance. The second equality follows from the commutativity of products of Toeplitz matrices with vectors where we have further defined the augmented matrices $\mathbf{h}_{sr}(n) = \left[\,\mathbf{h}_{sr,0}^{\mathrm{T}}(n),\ \ldots,\mathbf{h}_{sr,\mathrm{Q}}^{\mathrm{T}}(n)\,\right]^{\mathrm{T}}$ and $\boldsymbol{\Phi}(n) = \left[\,\mathbf{D}(w_0)\,\mathbf{U}(n),\ \ldots,\mathbf{D}\left(w_{\mathrm{Q}}\right)\mathbf{U}(n)\,\right]$, with $\mathbf{U}$ denoting the lower triangular Toeplitz matrix.

Similarly, the received signal at the destination can be written as

$$\mathbf{y}_{sd}(n) = \sqrt{E_s}\,\boldsymbol{\Phi}(n)\,\mathbf{h}_{sd}(n) + \mathbf{n}_{sd}(n) \tag{5}$$

where $\mathbf{h}_{sd}(n) = \left[\,\mathbf{h}_{sd,0}^{\mathrm{T}}(n),\ \ldots,\mathbf{h}_{sd,\mathrm{Q}}^{\mathrm{T}}(n)\,\right]^{\mathrm{T}}$ and $\mathbf{n}_{sd}(n)$ is the AWGN vector with entries of zero mean and $N_0/2$ variance.

During the relaying phase, the relay-received signals are fed to the ML detector[3] given by

$$\arg\min_{\bar{\mathbf{s}}} \left\{ \left\| \mathbf{y}_{sr}(n) - \sqrt{G_{sr}E_s} \sum_{q=0}^{\mathrm{Q}} \mathbf{D}(w_q)\mathbf{H}_{sr,q}^{(0)}(n)\,\boldsymbol{\Theta}\bar{\mathbf{s}} \right\|^2 \right\} \tag{6}$$

with $\bar{\mathbf{s}}$ is the set of all the possible signal block combinations. We implement "ideal DF" at the relay [25]. The relay then forwards a fresh decoded copy of the received pre-coded signal, i.e., $\dot{\mathbf{u}}(n)$. The received signal during the relaying phase at destination is then

$$\mathbf{y}_{rd}(n) = \sqrt{G_{rd}E_s}\,\dot{\boldsymbol{\Phi}}(n)\,\mathbf{h}_{rd}(n) + \mathbf{n}_{rd}(n) \tag{7}$$

[3] ML detection requires an exhaustive search with high complexity (exponential in the block length N_t). A relatively less complex near-ML search is provided by the sphere-decoding algorithm [26].

where $\mathbf{n}_{rd}(n)$ is the associated R → D AWGN vector with entries of zero mean and $N_0/2$ variance, $\dot{\mathbf{\Phi}}(n) = [\mathbf{D}(w_0)\dot{\mathbf{U}}(n) \cdots \mathbf{D}(w_Q) \cdot \dot{\mathbf{U}}(n)]$. Arranging (5) and (7) in matrix form

$$\mathbf{Y}(n) = \sqrt{E_s}\mathbf{S}(n)\,\mathbf{h}(n) + \mathbf{n}(n) \tag{8}$$

where $\mathbf{Y}(n) = \left[\, \mathbf{y}_{sd}(n) \;\; \mathbf{y}_{rd}(n) \,\right]^{\mathrm{T}}$, $\mathbf{S}(n) = \mathrm{diag}\left(\mathbf{\Phi}(n),\ \sqrt{G_{rd}}\dot{\mathbf{\Phi}}(n)\right)$, $\mathbf{h}(n) = \left[\, \mathbf{h}_{sd}(n) \;\; \mathbf{h}_{rd}(n) \,\right]^{\mathrm{T}}$ and $\mathbf{n}(n) = \left[\, \mathbf{n}_{sd}(n) \;\; \mathbf{n}_{rd}(n) \,\right]^{\mathrm{T}}$. The received signals are then fed to an ML detector.

For the multiple antenna deployment we adopt the coding scheme in Table 1. During the first transmission phase (broadcasting-1), the source vehicle broadcasts two pre-coded blocks, $\mathbf{u}(n-1) = \mathbf{\Theta}\mathbf{s}(n-1)$ and $\mathbf{u}(n) = \mathbf{\Theta}\mathbf{s}(n)$, from the first and second antennas, respectively. During the second transmission phase (broadcasting-2), the source vehicle broadcasts another version of the two pre-coded blocks, $\mathbf{u}^*(n) = -\mathbf{\Theta}\mathbf{s}^*(n)$ and $\mathbf{u}^*(n-1) = \mathbf{\Theta}\mathbf{s}^*(n-1)$, from the first and second antennas, respectively.

$$\mathbf{Y}(n) = \begin{matrix}[\mathbf{y}_{sd,1}(n-1) & \mathbf{y}_{sd,2}(n-1) & \mathbf{y}_{sd,1}(n) & \mathbf{y}_{sd,2}(n) \\ \mathbf{y}_{rd,1}(n-1) & \mathbf{y}_{rd,2}(n-1) & \mathbf{y}_{rd,1}(n) & \mathbf{y}_{rd,2}(n)]^{\mathrm{T}}\end{matrix}, \tag{9}$$

$$\mathbf{n}(n) = \begin{matrix}[\mathbf{n}_{sd}^{(1)}(n-1) & \mathbf{n}_{sd}^{(2)}(n-1) & \mathbf{n}_{sd}^{(1)}(n) & \mathbf{n}_{sd}^{(2)}(n) \\ \mathbf{n}_{rd}^{(1)}(n-1) & \mathbf{n}_{rd}^{(2)}(n-1) & \mathbf{n}_{rd}^{(1)}(n) & \mathbf{n}_{rd}^{(2)}(n)]^{\mathrm{T}}\end{matrix}, \tag{10}$$

$$\mathbf{h}_a(n) = \begin{matrix}[\,\mathbf{h}_{sd}^{(a,1)}(n-1) & \mathbf{h}_{sd}^{(a,2)}(n-1) & \left(\mathbf{h}_{sd}^{(a,1)}(n)\right)^* & \left(\mathbf{h}_{sd}^{(a,2)}(n)\right)^* \\ \mathbf{h}_{rd}^{(a,1)}(n-1) & \mathbf{h}_{rd}^{(a,2)}(n-1) & \left(\mathbf{h}_{rd}^{(a,1)}(n)\right)^* & \left(\mathbf{h}_{rd}^{(a,2)}(n)\right)^* \,]^{\mathrm{T}},\end{matrix} \tag{11}$$

$$\mathbf{S}_1(n) = \mathrm{diag}\left(\mathbf{\Phi}^{(1,1)}(n-1),\ \mathbf{\Phi}^{(1,2)}(n-1),\ -\mathbf{\Phi}^{(1,1)}(n),\ -\mathbf{\Phi}^{(1,2)}(n),\ \sqrt{G_{rd}}\dot{\mathbf{\Phi}}^{(1,1)}(n-1),\ \sqrt{G_{rd}}\dot{\mathbf{\Phi}}^{(1,2)}(n-1),\ -\sqrt{G_{rd}}\dot{\mathbf{\Phi}}^{(1,1)}(n),\ -\sqrt{G_{rd}}\dot{\mathbf{\Phi}}^{(1,2)}(n)\right), \tag{12}$$

and

$$\mathbf{S}_2(n) = \mathrm{diag}\left(\mathbf{\Phi}^{(2,1)}(n),\ \mathbf{\Phi}^{(2,2)}(n),\ \mathbf{\Phi}^{(2,1)}(n-1),\ \mathbf{\Phi}^{(2,2)}(n-1),\ \sqrt{G_{rd}}\dot{\mathbf{\Phi}}^{(2,1)}(n),\ \sqrt{G_{rd}}\dot{\mathbf{\Phi}}^{(2,2)}(n),\ \sqrt{G_{rd}}\dot{\mathbf{\Phi}}^{(2,1)}(n),\ \sqrt{G_{rd}}\dot{\mathbf{\Phi}}^{(2,2)}(n)\right) \tag{13}$$

In the third and fourth transmission phases (relaying-1/2), the relay first scales the received signal and then forwards the resulting signal to the destination. We re-define the entries in (8) as $\mathbf{S}(n) = \mathrm{diag}\left(\mathbf{S}_1(n),\ \mathbf{S}_2(n)\right)$ and $\mathbf{h}(n) = [\mathbf{h}_1(n) \;\; \mathbf{h}_2(n)]^{\mathrm{T}}$, with $\mathbf{Y}(n)$, $\mathbf{n}(n)$, $\mathbf{h}_a(n)$, $\mathbf{S}_1(n)$ and $\mathbf{S}_2(n)$ respectively defined in (9), (10), (11), (12) and (13). Note that $a, b \in \{1, 2\}$.

3. Performance gain analysis (PEP, diversity gains and outage probability)

In this section, we investigate the achievable diversity gain for our dual-phase dual-hop pre-coded MIMO cooperative schemes through the derivation of the PEP. Define $\gamma = E_s/N_0$ as the signal-to-noise ratio (SNR). After dropping the block indices $n-1$ and n in (8) for convenience of the presentation, the exact PEP is given by (14) [21] and the $\mathbf{S}$ matrix that holds the transmitted data information is now represented in terms of $\mathbf{S}_1$ and $\mathbf{S}_2$ defined earlier. Using the pre-coder $\mathbf{\Theta}$ to overcome the channel selectivity, we can justifiably assume that channel state information (CSI) is available at the relay and receiver sides. Let $\hat{\mathbf{S}}$ represent the erroneously decoded data matrix instead of the originally transmitted $\mathbf{S}$

$$P(\mathbf{S} \to \hat{\mathbf{S}} \,|\, \mathbf{h}) = \mathrm{Q}\left(\sqrt{\frac{E_s}{2N_0} d^2\left(\mathbf{S}, \hat{\mathbf{S}} \,|\, \mathbf{h}\right)}\right) \tag{14}$$

in the above, the Euclidean distance conditioned on the fading channel coefficients is $d^2\left(\mathbf{S} \to \hat{\mathbf{S}} \,|\, \mathbf{h}\right) = \mathbf{h}_1^{\mathrm{H}}\boldsymbol{\chi}_1\mathbf{h}_1 + \mathbf{h}_2^{\mathrm{H}}\boldsymbol{\chi}_2\mathbf{h}_2$ where $\boldsymbol{\chi}_1 = \left(\mathbf{S}_1 - \hat{\mathbf{S}}_1\right)^{\mathrm{H}}\left(\mathbf{S}_1 - \hat{\mathbf{S}}_1\right)$ and $\boldsymbol{\chi}_2 = \left(\mathbf{S}_2 - \hat{\mathbf{S}}_2\right)^{\mathrm{H}}\left(\mathbf{S}_2 - \hat{\mathbf{S}}_2\right)$. We can rewrite (14) as

$$P(\mathbf{S} \to \hat{\mathbf{S}} \,|\, \mathbf{h}) = \mathrm{Q}\left(\sqrt{\frac{E_s}{2N_0}\left(\mathbf{h}_1^{\mathrm{H}}\boldsymbol{\chi}_1\mathbf{h}_1 + \mathbf{h}_2^{\mathrm{H}}\boldsymbol{\chi}_2\mathbf{h}_2\right)}\right). \tag{15}$$

3.1. Pair-wise Error Probability (PEP) and diversity gains

Using the lower bound of the recent result in Ref. [27], (14) can be tightly lower bounded by

$$P\left(\mathbf{S} \to \hat{\mathbf{S}} \,|\, \mathbf{h}\right) \approx \sum_{m=1}^{3} \varepsilon_m \exp\left(-\rho_m \tfrac{E_s}{4N_0}\left(\mathbf{h}_1^{\mathrm{H}}\boldsymbol{\chi}_1\mathbf{h}_1 + \mathbf{h}_2^{\mathrm{H}}\boldsymbol{\chi}_2\mathbf{h}_2\right)\right) \tag{16}$$

where $\varepsilon_1 = \varepsilon_2 = 2\varepsilon_3 = 1/12$, $\rho_1 = 12\left(\sqrt{3}-1\right)/\pi$, $\rho_2 = 4\left(3-\sqrt{3}\right)/\pi$ and $\rho_3 = 2\sqrt{3}/\pi$.

$$\begin{aligned} P\left(\mathbf{S} \to \hat{\mathbf{S}} \,|\, \mathbf{h}\right) \le\ & P_{Coop}\left(\mathbf{S} \to \hat{\mathbf{S}} \,|\, \mathbf{h}_{sd}^{(a,b)}(n-1), \mathbf{h}_{sd}^{(a,b)}(n), \mathbf{h}_{rd}^{(a,b)}(n-1), \mathbf{h}_{rd}^{(a,b)}(n)\right) \\ & + P_{sr}\left(\mathbf{S} \to \hat{\mathbf{S}} \,|\, \mathbf{h}_{sr}^{(a,b)}(n-1), \mathbf{h}_{sr}^{(a,b)}(n)\right) P_{sd}\left(\mathbf{S} \to \hat{\mathbf{S}} \,|\, \mathbf{h}_{sd}^{(a,b)}(n-1), \mathbf{h}_{sd}^{(a,b)}(n)\right) \end{aligned} \tag{17}$$

$$P\left(\mathbf{S} \to \hat{\mathbf{S}} \,|\, \mathbf{h}\right) \le \psi_{sd}\left(\psi_{sr} + \psi_{rd}\right), \tag{18}$$

$$\psi_{sd} = \sum_{m=1}^{3} \varepsilon_m \exp\left(-\rho_m \left\{ \sum_{a=1}^{2}\sum_{b=1}^{2} \left(\left(\mathbf{h}_{sd}^{(a,b)}(n-1)\right)^{\mathrm{H}} \boldsymbol{\chi}_a \times \mathbf{h}_{sd}^{(a,b)}(n-1) + \left(\mathbf{h}_{sd}^{(a,b)}(n)\right)^{\mathrm{H}} \boldsymbol{\chi}_b \mathbf{h}_{sd}^{(a,b)}(n) \right) \right\} \frac{1}{4}\gamma \right),$$

$$\psi_{sr} = \sum_{m=1}^{3} \varepsilon_m \exp\left(-\rho_m \left\{ \sum_{a=1}^{2}\sum_{b=1}^{2} \left(\left(\mathbf{h}_{sr}^{(a,b)}(n-1)\right)^{\mathrm{H}} \boldsymbol{\chi}_a \times \mathbf{h}_{sr}^{(a,b)}(n-1) + \left(\mathbf{h}_{sr}^{(a,b)}(n)\right)^{\mathrm{H}} \boldsymbol{\chi}_b \mathbf{h}_{sr}^{(a,b)}(n) \right) \right\} \frac{1}{4}\gamma \right)$$

and

$$\psi_{rd} = \sum_{m=1}^{3} \varepsilon_m \exp\left(-\rho_m \left\{ \sum_{a=1}^{2}\sum_{b=1}^{2} \left(\left(\mathbf{h}_{rd}^{(a,b)}(n-1)\right)^{\mathrm{H}} \boldsymbol{\chi}_a \times \mathbf{h}_{rd}^{(a,b)}(n-1) + \left(\mathbf{h}_{rd}^{(a,b)}(n)\right)^{\mathrm{H}} \boldsymbol{\chi}_b \mathbf{h}_{rd}^{(a,b)}(n) \right) \right\} \frac{1}{4}\gamma \right)$$

As mentioned, the relay decides that an incorrect decision has been made through CRC deployment, and then forward a fresh copy of the pre-coded signal to destination only if the signal is decoded correctly. Hence, for DF cooperative relaying, the pair-wise error probability after some mathematical manipulation will follow the PEP expression in [25] (shown in (17)). With $a, b \in \{1, 2\}$, where $P_{Coop}(.)$ is the PEP for the relay selection cooperative transmission, $P_{sr}(.)$ is the PEP for the S → R and $P_{sd}(.)$ is the error probability of S → D link. After some mathematical manipulations and by evaluating $P_{Coop}(.)$, $P_{sr}(.)$ and $P_{sd}(.)$, (17) can be rewritten as (18).

We need to average (18) over $\mathbf{h}$. Using the eigenvectors decomposition and following a similar analysis to that in [28] for the channel vectors, then $\gamma_{sd}^{(a,b)}(.) = \left(\mathbf{h}_{sd}^{(a,b)}(.)\right)^{\mathrm{H}} \boldsymbol{\chi}_a \mathbf{h}_{sd}^{(a,b)}(.) +$

$\left(\mathbf{h}_{sd}^{(a,b)}(.)\right)^{\mathrm{H}} \boldsymbol{\chi}_b \mathbf{h}_{sd}^{(a,b)}(.) = 2\sum_{k=0}^{r_{sd}-1} \alpha_k^{(a,b)}(.)\,|\beta_k^{sd}(.)|^2$ is the eigenvector for the normalized S → D channel vector and $[\beta_0^{sd}, \beta_1^{sd}, \ldots, \beta_{r_{sd}-1}^{sd}]$ is associate channel gain vector for the normalized S → D. Similarly define $\gamma_{sr}(.)$ and $\gamma_{rd}(.)$, with $r_{sr}^{(a,b)} = (L_{sr}^{(a,b)}+1)(Q_{sr}^{(a,b)}+1)$ and $r_{rd}^{(a,b)} = (L_{rd}^{(a,b)}+1)(Q_{rd}^{(a,b)}+1)$ as the associated links ranks for the S → R and R → D, respectively. $[\kappa_0, \kappa_1, \ldots, \kappa_{sr-1}]$ and $[\delta_0, \delta_1, \ldots, \delta_{rd-1}]$ are the eigenvectors for the associated links, and $[\beta_0^{sr}, \beta_1^{sr}, \ldots, \beta_{r_{sr}-1}^{sr}]$ and $[\beta_0^{rd}, \beta_1^{rd}, \ldots, \beta_{r_{rd}-1}^{rd}]$ are the channel gain vectors for the associated links. Inserting this into (18) and averaging with respect to β_k^{sd}, β_k^{sr} and β_k^{rd} which follow a Rayleigh distribution, we can obtain the unconditional PEP as (19). At relatively high SNR, we observe from (19) that an asymptotic diversity gain of

$$P\left(\mathbf{S}\to\hat{\mathbf{S}}\right) \le \prod_{a=1}^{2}\prod_{b=1}^{2}\left(\prod_{p=0}^{r_{sd}^{(a,b)}-1}\left(1+\frac{\alpha_p^{(a,b)}}{4}\gamma\right)^{-1}\right) \times \left(\prod_{a=1}^{2}\prod_{b=1}^{2}\left(\prod_{p=0}^{r_{sr}^{(a,b)}-1}\left(1+\frac{\kappa_p^{(a,b)}}{4}\gamma\right)^{-1}\right)\right. + \left.\prod_{a=1}^{2}\prod_{b=1}^{2}\left(\prod_{p=0}^{r_{rd}^{(a,b)}-1}\left(1+\frac{\delta_p^{(a,b)}}{4}\gamma\right)^{-1}\right)\right) \quad (19)$$

$$D_{gain} = \sum_{a=1}^{2}\sum_{b=1}^{2} r_{sd}^{(a,b)} + \min\left(\sum_{a=1}^{2}\sum_{b=1}^{2} r_{sr}^{(a,b)}, \sum_{a=1}^{2}\sum_{b=1}^{2} r_{rd}^{(a,b)}\right) \quad (20)$$

is available. From (20), we observe that the maximum asymptotic diversity gain is bounded by the rank of the auto-correlation matrix associated with the direct link between the BS and the designated vehicle (S → D) and the minimum of the cooperative relaying links (S → R and R → D), taking into consideration the number of transmit and receive antennas involved in the transmission. If the relative travelling velocity of relaying vehicle with respect to the designated vehicle is not equal to zero, extra diversity gains can be extracted from the S → R → D link.

3.2. Outage probability

Wireless transmission is constrained by a regulated transmission power, which limits the coverage area. We show that using cooperative transmission can improve the quality of received signal, in addition to extending the coverage area. The outage probability P_{out} is the probability that the error probability exceeds a specified value $\dot{\gamma}_{th}$, i.e., $P_{out} = \int_0^{\dot{\gamma}_{th}} f_{\dot{\gamma}}(\dot{\gamma})\,d\dot{\gamma}$ [29] is the cumulative distribution function (CDF) of $\dot{\gamma}$, namely $F_{\dot{\gamma}}(\dot{\gamma}_{th})$. By defining our un-normalized aggregate channel model which takes into account both path-loss and small-scale fading, the relative geometrical gains are re-defined as $G_{sd} = d_{sd}^{-\alpha}$, $G_{sr} = d_{sr}^{-\alpha}$ and $G_{rd} = d_{rd}^{-\alpha}$. These can be related to one another through the cosine theorem $G_{sr}^{-2/\alpha} + G_{rd}^{-2/\alpha} - 2G_{sr}^{-1/\alpha}G_{rd}^{-1/\alpha}\cos\theta = G_{sd}^{-2/\alpha}$, and assuming a normalized gain for a 1 m distance [30]. From (19) and the definition of CDF, the outage probability is given by (21).

$$P_{out} \le \prod_{a=1}^{2}\prod_{b=1}^{2}\left(\prod_{p1=0}^{r_{sd}^{(a,b)}-1}\prod_{p2=0}^{r_{sr}^{(a,b)}-1}\left(\frac{\log\left(\frac{4+\alpha_{p1}^{(a,b)}}{4+\kappa_{p2}^{(a,b)}}\right)}{\left(\frac{\alpha_{p1}^{(a,b)}-\kappa_{p2}^{(a,b)}}{4}\right)\dot{\gamma}_{th}}\right)\right.$$

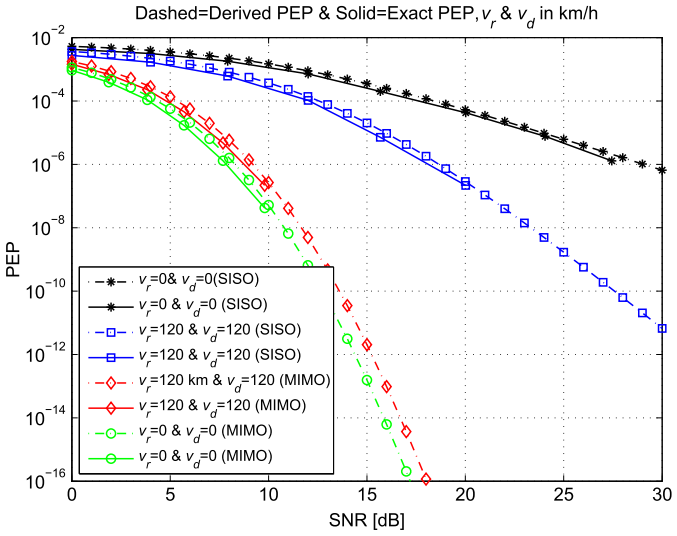

Fig. 3. Comparison of the derived PEP in (19) and the exact PEP for the MIMO scheme.

$$+\left.\prod_{p1=0}^{r_{sd}^{(a,b)}-1}\prod_{p2=0}^{r_{rd}^{(a,b)}-1}\left(\frac{\log\left(\frac{4+\alpha_{p1}^{(a,b)}}{4+\delta_{p2}^{(a,b)}}\right)}{\left(\frac{\alpha_{p1}^{(a,b)}-\delta_{p2}^{(a,b)}}{4}\right)\dot{\gamma}_{th}}\right)\right) \quad (21)$$

As earlier defined in section 3.1, the entries in (21) $\alpha_p^{(a,b)}$, $\kappa_p^{(a,b)}$ and $\delta_p^{(a,b)}$ are the eigenvalues that model the $\boldsymbol{\chi}_1$ and $\boldsymbol{\chi}_2$ vectors. Recall that $\boldsymbol{\chi}_1 = \left(S_1 - \hat{S}_1\right)^{\mathrm{H}}\left(S_1 - \hat{S}_1\right)$ and $\boldsymbol{\chi}_2 = \left(S_2 - \hat{S}_2\right)^{\mathrm{H}}\left(S_2 - \hat{S}_2\right)$. From the definitions of the entries in (8) we find that $\mathbf{S}(n) = \mathrm{diag}(S_1(n), S_2(n))$ holds the values of G_{sd}, G_{sr} and G_{rd}, i.e. the relative geometrical gains for the S → D, S → R, and R → D links, respectively, which is a function of the underlying links distances d_{sd}, d_{sr} and d_{rd}.

4. Numerical and simulation results

In this section, we investigate the performance of cooperative vehicular relaying over doubly-selective fading channel and double-ring second-order statistics deploying our modified 2 × 2-Alamouti MIMO antenna configuration. We demonstrate the performance gains of the proposed scheme using numerical results from our mathematical model and Matlab Monte-Carlo simulations. As defined in the standard, LTE-A targets peak data rates up to 1 Gb/s with up to 100 MHz supported spectrum bandwidth and QPSK modulation is used [31]. Unless otherwise stated, we consider $f_c = 2.5$ GHz, $T_s = 500$ μs, $v_r = v_d = 120$ km/h, $\alpha = 3.67$, $\theta = \pi$ and $\tau_d = 1.328$ μs [8]. The relative geometrical gain is $G_{sr}/G_{rd} = -30$ dB, and indicates that the relay is close to the destination. We assume CSI is available at the receiving terminals. We use the pre-coder $\boldsymbol{\Theta}$ with parameters $P = 2$ and $Z = 2$. This results in $[L_{sd}, Q_{sd}] = [1, 1]$ for S → D link. Due to the zero relative velocity for the R → D link, a frequency-time flat channel is used, hence $[L_{coop}, Q_{coop}] = [0, 0]$. Based on the system parameters stated above, we result in a transmission duration of ≈ 48 s before the relaying vehicle travels away from the base station location. With 100–150 Mbps downlink data rate supported for high mobility by LTE-A technology, our scheme is capable of transferring large data messages. Large messages/streaming sizes can be divided into data chunks and distributed over several cooperative relaying links.

In Fig. 3, we verify our analytical derivations by comparing the derived PEP expressions in (19) with the exact PEP expres-

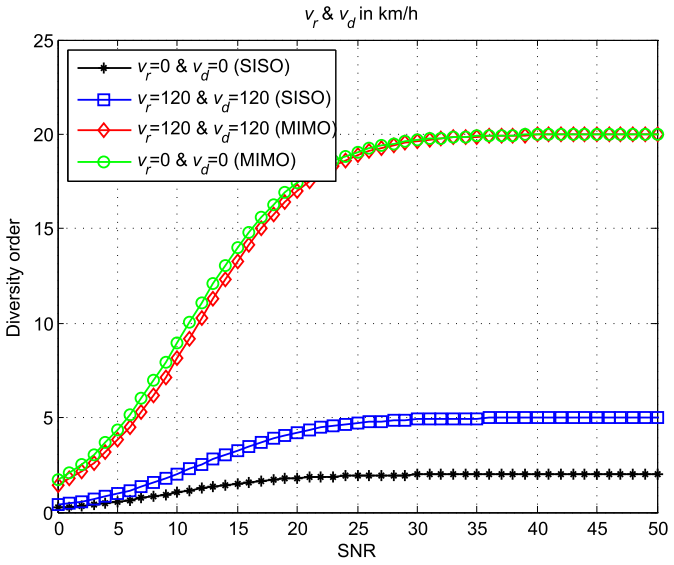

Fig. 4. Diversity order of the MIMO cooperative relaying scheme for an LTE-A downlink session.

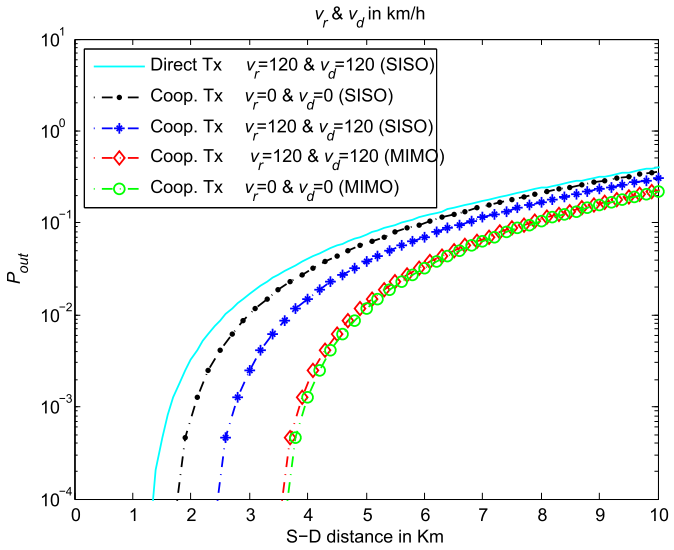

Fig. 5. S → D distance in km versus outage probability.

sions. Two benchmark conditions are considered, the first is the case of perfect stationary terminals with single antenna deployments at all nodes. The second is for perfect stationary terminals with a 2×2-MIMO deployment between the eNodeB/BS and designated end vehicle. In both cases we have $v_r = v_d = 0$ km/h, i.e. $[L_{sd}, Q_{sd}] = [L_{coop}, Q_{coop}] = [0, 0]$. A single antenna is used at the relaying vehicle. Exact PEP can be found by taking the expectation numerically for (15) [21], through random generation of all the underlying $\mathbf{h}_{sd}$, $\mathbf{h}_{sr}$ and $\mathbf{h}_{rd}$ links, and using proper statistics via numerical techniques. In the broadcasting phase, the source (antenna) transmits its pre-coded signal to the relaying vehicle and to the designated vehicle. In the relaying phase, the relay is engaged in forwarding the received signal only if it was decoded correctly, otherwise the relay is silent. The destination makes its decision based on the two received signals over the broadcasting and relaying phases. The relay then forward a fresh copy of the pre-coded signal to destination. We assume perfect CSI at the receiver side, and present the performance of MIMO cooperative transmission. A power consumption saving is clearly observed, note that as the values of (L) and/or (Q) increase, significant improvements are observed through precoding which takes advantages of diversity gains. For example at a target pairwise error rate of 10^{-5}, the pre-coded system over a channel with $v_r = v_d = 120$ km/h (with a single antenna deployment and $L = 1$ and $Q = 1$) is 7 dB superior to the benchmark curve of $v_r = v_d = 0$ km/h (with a single antenna deployment and $L = 0$ and $Q = 0$). The benchmark curve indicates the non-pre-coded flat channels. Performance improvement climbs up to 17 dB for $v_r = v_d = 120$ km/h with our proposed transmission scheme (2×2 MIMO with Alamouti STBC and $L = 1$ and $Q = 1$). As shown in the figure our proposed scheme gives a tight equivalent performance to the ideal case with $v_r = v_d = 0$ km/h and a 2×2-Alamouti MIMO deployment.

In Fig. 4, we plot $-\log P\left(\mathbf{S} \to \hat{\mathbf{S}}\right)/\log(\gamma)$ to precisely observe the slope of the error performance curves. The achieved diversity orders are consistent with equation (20), and equal to $D_{gain,R} = 20$, compared to $D_{gain,R} = 2$ for traditional non-pre-coded cooperative relaying transmission and $D_{gain,R} = 5$ for the pre-coded cooperative relaying transmission with single antenna deployment. As shown in Fig. 4, our proposed transmission scheme achieves similar diversity gains compared to the ideal benchmark case with $v_r = v_d = 0$ km/h and a 2×2-Alamouti MIMO deployment. Even at lower SNR the ideal condition reaches the full diversity with only $\simeq 0.5$ dB lower than our proposed scheme. As shown in (20), the diversity gains and hence the over all system performance is directly proportional to the number of the deployed antennas at the eNodeB and the destination vehicle.

Fig. 5 shows the coverage extension gains for the opportunistic cooperative transmission compared to the direct transmission using the outage probabilities in (21), for $\gamma = 10$ dB and $\dot{\gamma}_{\text{th}} = 5$ dB [32]. For outage probability of 10^{-4}, coverage extension advantage of 0.3 km, 0.9 km, 2.1 km and 2.2 km is observed for cooperative transmission with $v_r = v_d = 0$ km/h (with single antenna deployment and $L = 0$ and $Q = 0$), $v_r = v_d = 120$ km/h (with single antenna deployment and $L = 1$ and $Q = 1$), $v_r = v_d = 120$ km/h (with a 2×2 MIMO using our modified Alamouti code and $L = 1$ and $Q = 1$), and $v_r = v_d = 0$ km/h (as the perfect benchmark performance, with a 2×2 MIMO using our modified Alamouti code and $L = 0$ and $Q = 0$), respectively, compared to traditional direct transmission with $v_r = v_d = 0$ km/h and single antenna deployment. We observe that our proposed scheme gives a close/tight performance to the perfect benchmark curve.

In our study we assume that the pre-coder parameters $P = 2$ and $Z = 2$. Hence the input data blocks $\mathbf{s}(n)$ is of length $N_s \times 1$ (i.e., PZ) and the output of the pre-coder $\mathbf{u}(n)$ is of length $N_t \times 1$ (i.e. $(P + Q)(Z + L)$). We then have the pre-coder output rate equal to $N_s/N_t = PZ/((P + Q)(Z + L))$. It is clear that increasing the pre-coder output rate can be achieved by increasing P and Z. This will be a trade-off with respect to the system complexity (mainly detection complexity), by increasing the transmitted/received block length. Furthermore, the diversity order is a function of the channel order $(Q + 1)(L + 1)$. From the definition of P and Z, we have $Q(1 - (Z + L)T_s f_d) - 1 < P(Z + L)T_s f_d \leq Q(1 - (Z + L)T_s f_d)$. Hence we can choose P and Z to satisfy a minimum required Q (i.e. as illustrated in Table 2).

Taking into consideration that we use an open loop outer pre-coding technique for signal transmission, ML coherent detection can be used with the aid of pilot symbol assisted modulation (PSAM) techniques to help retrieve the channel information. It is well known that non-coherent receiver needs less expensive and lower complexity circuits than ML coherent receivers on the cost of bit error rate performance [33]. However, because of the rapid advancing of hardware technologies, the cost and complexity issues notably decrease with time, which motivates us to focus on performance. In a specific study [33] for SISO mobile system with

Table 2
The number of Doppler shifts Q for a given block length and P–Z parameters.

$[P, Z]$	Q	Transmitted block length N_t	ML search possibilities. *m is the bits/symbol
[1, 1]	1	4	$(m)^4$
[13, 13]	2	210	$(m)^{210}$
[18, 18]	3	399	$(m)^{399}$
[22, 22]	4	598	$(m)^{598}$
[25, 25]	5	780	$(m)^{780}$
[18, 18]	6	986	$(m)^{986}$
[31, 31]	7	1216	$(m)^{1216}$

a doubly selective channels and one Doppler frequency, the coherent receivers needs 5 dB less SNR to achieve the same performance as non-coherent system. And even with the assumption of mismatched coherent systems, the BER performance of coherent system outperforms the non-coherent one in cooperative systems [34]. The aforementioned channel estimation technique, i.e., PSAM, uses distributed pilot pattern that can also be used in practice for synchronization purpose without additional cost.

As proven by the authors in their previous work [19], under the assumption of imperfect channel state information and for sufficiently high SNR, the error rate curves for the cooperative link becomes independent of the SNR and results in the presence of error floors. The error floor saturates the error curves, where the error rates remain constant without any further improvements even when increasing the transmitting power. However, extracting or imposing extra diversity gains will suppress the error floors in the simulated SNR to lower levels.

5. Conclusion and future work

We propose a physical layer enabling scheme using cooperative-MIMO transmission and DF relaying. Our scheme makes use of on-road vehicles equipped with low elevation antennas to relay signals for LTE-A downlink sessions between eNodeB and a designated end vehicle through a highway traffic. We deploy a modified 2×2-Alamouti STBC to ensure the orthogonality of the MIMO transmitted/received signals and to benefit from the multiple antenna maximum diversity gains. A pre-coded DPS is used to mitigate the effect of the channel selectivity and to extract the rich inherent multipath-Doppler diversity. As benchmarks to assess our analysis and future research studies of such an approach, through the derivation of a lower bound expression of pairwise error probability (PEP), we analyze the achievable error rates, the diversity gains, and further we derive the outage probability closed-form expression. Our analytical and simulation results demonstrate that in broadband cellular networks, cooperative-MIMO using proper coding and vehicles as relays does not only potentiate improved levels of error rates performance associated with lower power consumption, but also provides higher diversity gains and increased coverage compared to conventional transmission schemes. Results also show that our transmission scheme can achieve performance that is tightly compliant to that of the ideal stationary flat-fading scenarios even under high mobility and selective fading.

In addition to our modified 2×2-Alamouti STBC, as a future work we envision the use of more than two antennas at both the transmitter and receiver with a higher orders of STBCs. This can be attained by using extra relaying vehicles during each cooperative transmission phase or by extending the cooperative transmission to more than the two transmission phases (used in this paper). Proper deployment of higher space–time block codes is expected to result in better error rates, higher diversity gains and improved coverage distances.

References

[1] J.M. Moualeu, W. Hamouda, X. HongJun, F. Takawira, Multi-relay turbo-coded cooperative diversity networks over Nakagami-m fading channels, IEEE Trans. Veh. Technol. 62 (9) (Nov. 2013) 4458–4470.

[2] J. Haghighat, W. Hamouda, Decode–compress-and-forward with selective-cooperation for relay networks, IEEE Commun. Lett. 16 (3) (Mar. 2012) 378–381.

[3] M. Kalil, A. Shami, A. Al-Dweik, QoS-aware power-efficient scheduler for LTE uplink, IEEE Trans. Mob. Comput. 99 (Oct. 2014) 1672–1685.

[4] D.J. Dechene, A. Shami, Energy-aware resource allocation strategies for LTE uplink with synchronous HARQ constraints, IEEE Trans. Mob. Comput. 13 (2) (Feb. 2014) 422–433.

[5] D.J. Dechene, A. Shami, Energy efficient quality of service traffic scheduler for MIMO downlink SVD channels, IEEE Trans. Wirel. Commun. 9 (12) (Dec. 2010) 3750–3761.

[6] C.X. Wang, X. Cheng, D. Laurenson, Vehicle-to-vehicle channel modeling and measurements: recent advances and future challenges, IEEE Commun. Mag. 47 (11) (Nov. 2009) 96–103.

[7] G. Acosta, K. Tokuda, M.A. Ingram, Measured joint Doppler-delay power profiles for vehicle-to-vehicle communications at 2.4 GHz, in: IEEE Global Telecomm. Conf., GlobeCom, Dallas, TX, Nov. 2004, pp. 3813–3817.

[8] I. Sen, D. Matolak, Vehicle-to-vehicle channel models for the 5-GHz band, IEEE Trans. Intell. Transp. Syst. 9 (June 2008) 235–245.

[9] S. Cheng, G. Horng, C. Chou, Adaptive vehicle-to-vehicle heterogenous transmission in cooperative cognitive network VANETs, Int. J. Innov. Comput. Inf. Control 8 (2) (Feb. 2012) 1263–1274.

[10] H. Zhang, N. Prasad, S. Rangarajan, MIMO downlink scheduling in LTE systems, in: IEEE Int. Conf. Comput. Commun., INFOCOM, Orlando, FL, Apr. 2012, pp. 2936–2940.

[11] Q. Wang, P. Fan, K.B. Letaief, On the joint V2I and V2V scheduling for cooperative VANETs with network coding, IEEE Trans. Veh. Technol. 61 (1) (Jan. 2012) 62–73.

[12] N. Adhikari, S. Noghanian, Multiple antenna systems for vehicle to vehicle communications, in: IEEE Intl. Conf. Electro/Information Technol, EIT, Rapid City, SD, May 2013, pp. 1–6.

[13] A. Assra, W. Hamouda, A. Youssef, EM-based joint channel estimation and data detection for MIMO-CDMA systems, IEEE Trans. Veh. Technol. 59 (3) (Mar. 2010) 1205–1216.

[14] S.M. Alamouti, A simple transmit diversity technique for wireless communications, IEEE J. Sel. Areas Commun. 16 (8) (Oct. 1998) 1451–1458.

[15] W. Hamouda, M. AlJerjawi, A transmit diversity scheme using space–time spreading for DS-CDMA systems in Rayleigh fading channels, in: IEEE Conf. Veh. Technol, VTC, Dallas, TX, Sept. 2005, pp. 147–151.

[16] G. Farhadi, N. Beaulieu, On the ergodic capacity of multi-Hop wireless relaying systems, IEEE Trans. Wirel. Commun. 8 (5) (May 2009) 2286–2291.

[17] Y. Fan, J. Thompson, MIMO configurations for relay channels: theory and practice, IEEE Trans. Wirel. Commun. 6 (5) (May 2007) 1774–1786.

[18] X. Ma, G. Leus, G.B. Giannakis, Space–time-Doppler block coding for correlated time-selective fading channels, IEEE Trans. Signal Process. 53 (6) (June 2005) 2167–2181.

[19] M.F. Feteiha, H.S. Hassanein, Enabling cooperative relaying VANET clouds over LTE-A networks, IEEE Trans. Veh. Technol. 64 (4) (Apr. 2015) 1468–1479.

[20] W.C. Jakes, Microwave Mobile Communications, Wiley-IEEE Press, New York, USA, 1994.

[21] J.G. Proakis, M. Salehi, Digital Communications, 5th ed., McGraw-Hill Inc., New York, NY, USA, 2008.

[22] A.S. Akki, F. Haber, A statistical model of mobile-to-mobile land communication channel, IEEE Trans. Veh. Technol. 35 (1) (Feb. 1986) 2–7.

[23] J.N. Laneman, G.W. Wornell, Distributed space–time-coded protocols for exploiting cooperative diversity in wireless networks, IEEE Trans. Inf. Theory 49 (10) (Oct. 2003) 2415–2425.

[24] X. Ma, G. Giannakis, Maximum-diversity transmissions over doubly selective wireless channels, IEEE Trans. Inf. Theory 49 (7) (July 2003) 1832–1840.

[25] Y. Ma, N. Yi, R. Tafazolli, Bit and power loading for OFDM-based three-node relaying communications, IEEE Trans. Signal Process. 56 (7) (July 2008) 3236–3247.

[26] O. Damen, A. Chkeif, J. Beltore, Lattice code decoder for space–time codes, IEEE Commun. Lett. 4 (5) (May 2000) 161–163.

[27] M. Wu, X. Lin, P.Y. Kam, New exponential lower bounds on the Gaussian Q-function via Jensen's inequality, in: IEEE 73rd Veh. Technol. Conf., VTC, Budapest, Hungary, May 2011, pp. 1–5.

[28] M.F. Feteiha, M. Uysal, Cooperative transmission for broadband vehicular networks over doubly-selective fading channels, IET Commun. 6 (16) (Nov. 2012) 2760–2768.

[29] M.K. Simon, M.S. Alouini, Digital Communication Over Fading Channels, Wiley-IEEE Press, 2005.

[30] S. Cui, A.J. Goldsmith, A. Bahai, Energy-constrained modulation optimization, IEEE Trans. Wirel. Commun. 4 (5) (Sept. 2005) 2349–2360.

[31] C. Zhang, S. Ariyavisitakul, M. Tao, LTE-advanced and 4G wireless communications [Guest Editorial], IEEE Commun. Mag. 50 (2) (Feb. 2012) 102–103.
[32] D.S. Michalopoulos, A.S. Lioumpas, G.K. Karagiannidis, R. Schober, Selective cooperative relaying over time-varying channels, IEEE Trans. Commun. 58 (8) (Aug. 2010) 2402–2412.
[33] A.M. Sayeed, B. Aazhang, Joint multipath-Doppler diversity in mobile wireless communications, IEEE Trans. Commun. 47 (1) (Jan. 1999) 123–132.
[34] H. Mheidat, M. Uysal, Non-coherent and mismatched-coherent receivers for distributed STBCs with amplify-and-forward relaying, IEEE Trans. Wirel. Commun. 6 (11) (Nov. 2007) 4060–4070.